PIXE and its applications to elemental analysis.

Ph.D. Maria Victoria Manso

Review presented for UESB webinars.

Schedule

- Introduction
- Interactions of heavy charged particles with electrons and atoms.
- Characteristic X-rays and Bremstrahlung production.
- X-ray detectors and Target preparation for PIXE.
- Experimental setup for PIXE (accelerators and chamber for target)
- Applications of PIXE to elemental analysis.
- Summary

IBA techniques

Elastic

. RBS
. ERDA (Elastic Recoil Detection Analysis)
.Nuclear Resonance

Inelastic

. PIXE
. PIGE
.NRA (Nuclear Reaction Analysis)

PIXE(1950) / Applications (1970-1980)

Chemistry, medicine, biology, agriculture, industry, environmental pollution, archeology, criminal investigations , and searches for mineral resources.

Heavy charged particles + atoms

Excitation: First Born Approximation (function of charge and velocity of projectile)

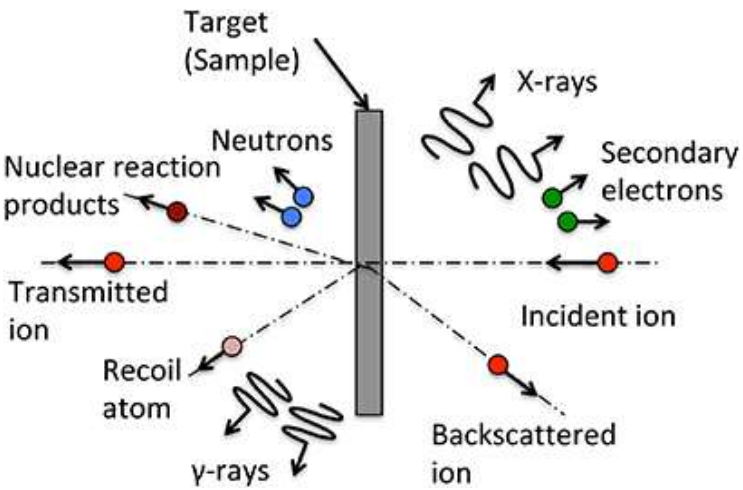

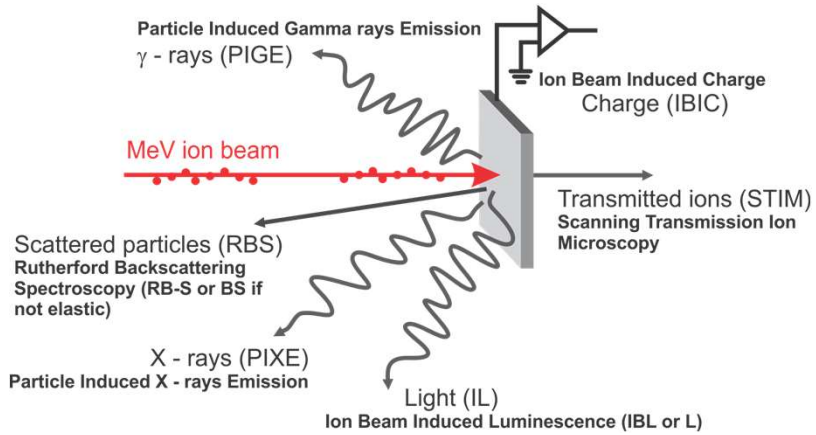

X-rays production in the sample.

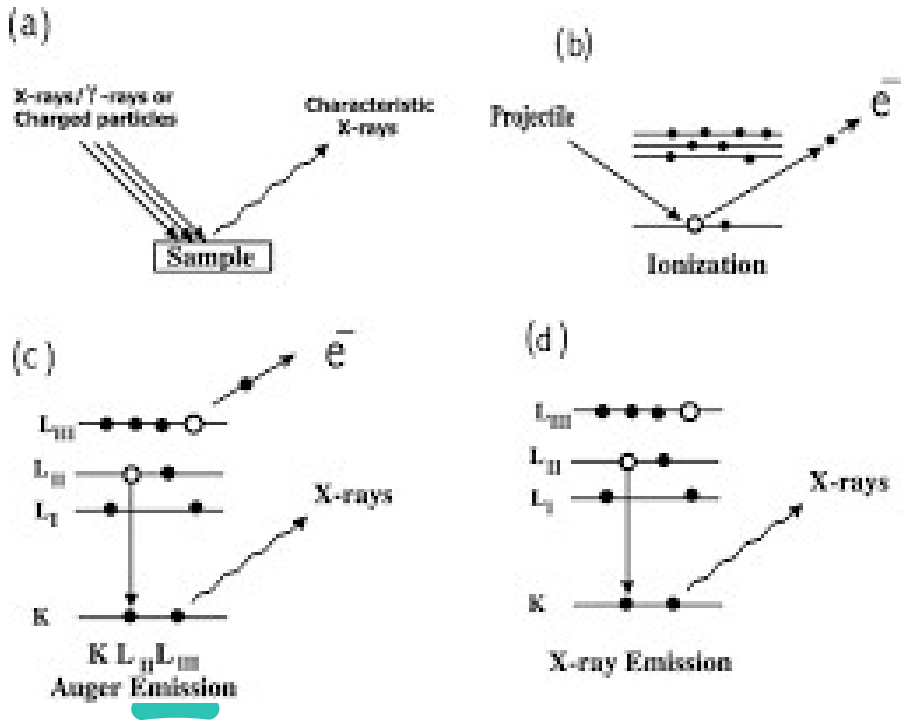

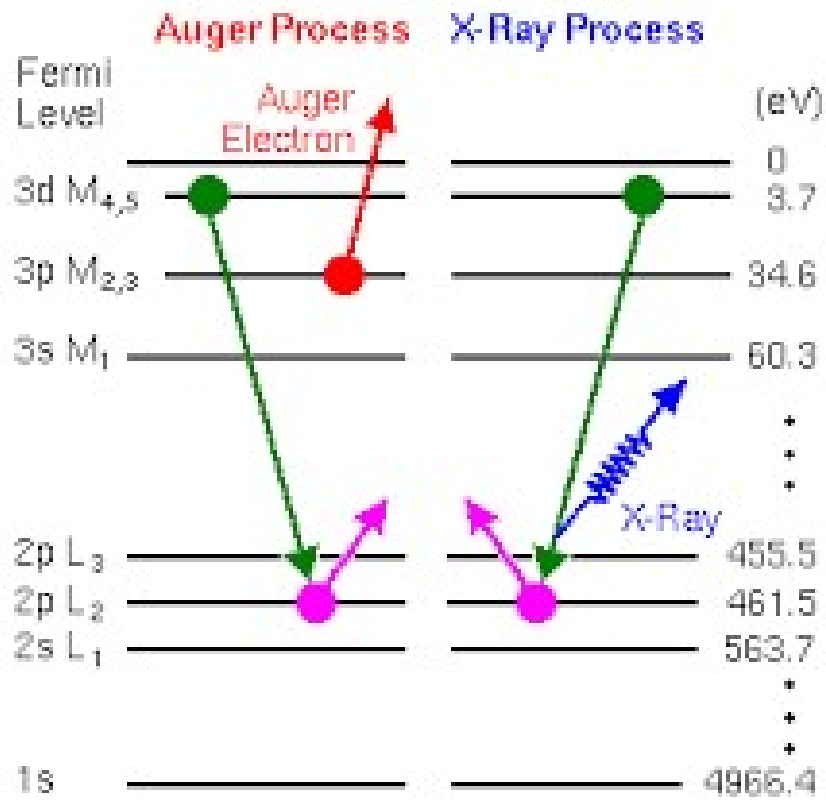

Notations (Siegbahn & IUPAC) of characteristic x rays

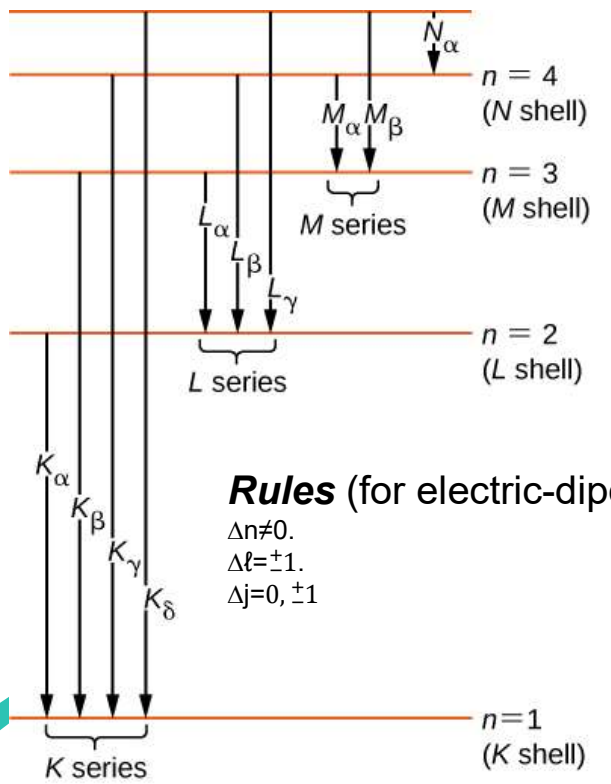

Rules (for electric-dipole)

$\Delta n \neq 0$.

$\Delta \ell = \pm 1$.

$\Delta j = 0, \pm 1$

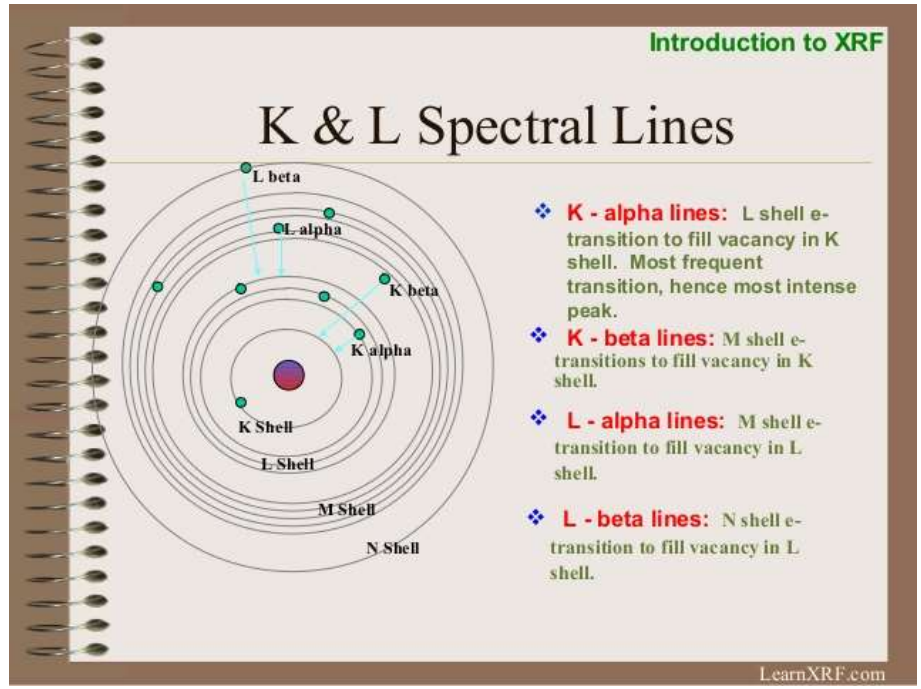

H, He, Li, Be have no-characteristic X-rays. However, new transitions become possible with the filling up the outer electron shells.

Inner shell ionization according to velocity of projectile

$V_p \approx v_e$

Rutherford Scattering
(closed collisions)

$V_p > v_e$

Projectile interacts with the cloud.
(distant collisions)

$V_p \approx c$

Photoelectric effect
(like interacts with a virtual photon)

Inner shell ionization energetic condition.

Electron is bound in an atom with an average energy :

$$-U = \frac{m.v^2}{2} - \frac{Z.e^2}{r}$$

In head-on collision(projectile +electron), the transfered energy from projectile to electron is:

$$\mathrm{E} = 2mV^2 + 2mvV$$

Therefore, the ionization condition is:

$$2mV^2 + 2mvV \geq U \Rightarrow v \geq \frac{U - 2mV^2}{2mV}$$

Always valid if:

$$U \geq 2mV^2$$

Electrons with large velocity are only ionized in the case of low velocity projectiles in the vicinity of the nucleus

Therefore, the inner shell ionization cross section drop with decreasing projectile energy, $\mathbf{T} = \frac{M.V^2}{2}$

Inner shell ionization energetic condition.

$$U \geq 2mV^2 |.(\frac{M}{2}) \rightarrow \frac{M}{4m} U = \frac{M}{2} V^2 \rightarrow E_{max} \sim \frac{4m}{M} T$$

$$\frac{4m}{M} T = 2mv^2 \rightarrow E_{electron} \sim \frac{m}{M} T$$

The ionization cross sections are maximized when the projectile velocity becomes the same as the average velocity of the bound electron.

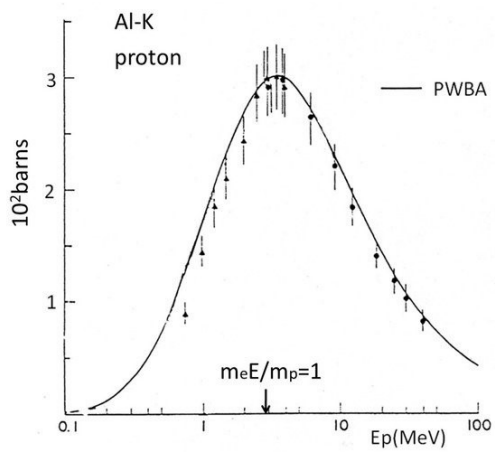

Fluorescence yield.

$$w_K = \frac{I_K}{N_k};$$ K -shell.

Where: I_K- is the total number of X-rays K emitted on the sample.
N_k-is the total number of vacancies on the K line.

L-shell and other fluorescence yield.

Very complicated because non-radiative transitions (COSTER_ KRONING) between sub-shells can occur.

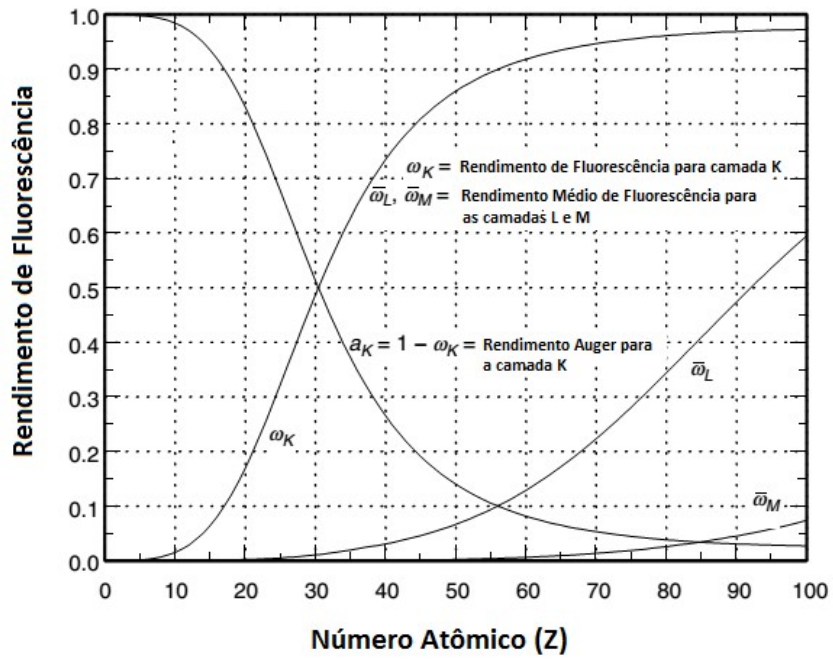

CONTINUOUS X-rays due ion-atom collisions

QUASI FREE ELECTRON BREMSSTRAHLUNG (QFEB)-

SECONDARY ELECTRON BREMSSTRAHLUNG (SEB)

ATOMIC BREMSSTRAHLUNG (AB)

Si(Li) semiconductor- Detection

Inelastic scattering between an energetic ion and a target atom can lead to inner shell ionization with the subsequent emission of an X-ray.

The energy of the x-ray, which is characteristic of the excited atom, is detected by a solid state Si(Li) detector.

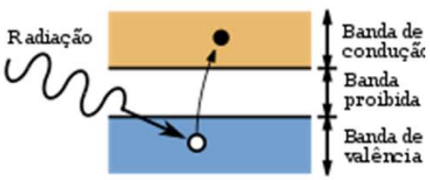

1 pair e-h for Si /3.62 eV of lost energy, at LN temperature.

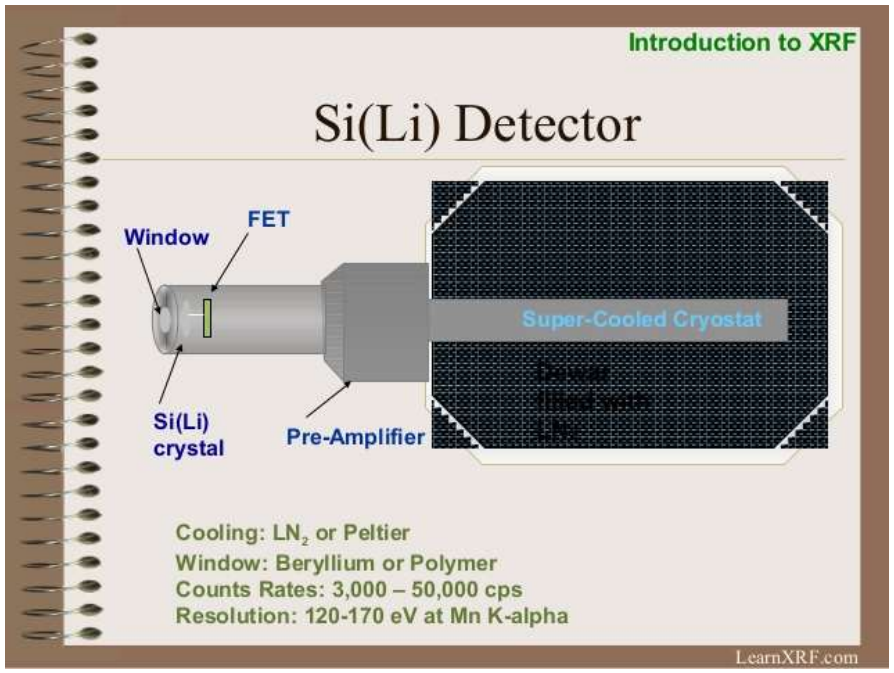

Compact detectors

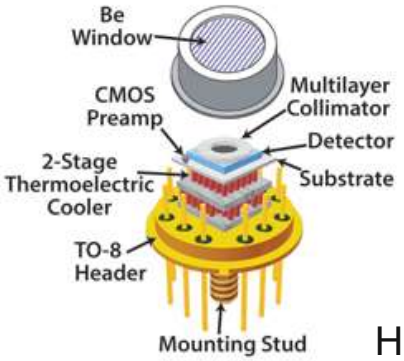

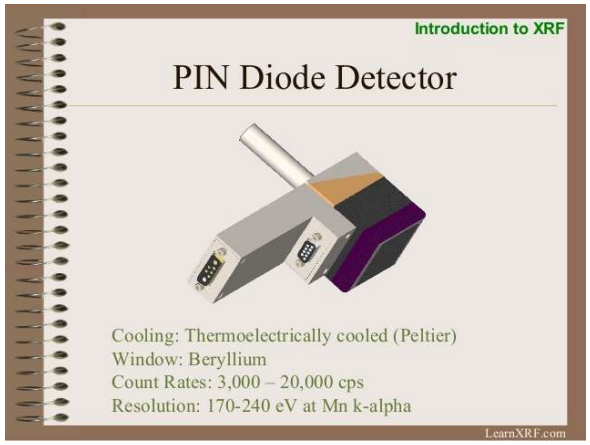

Heart - 2 stage thermoelectrically cooled Si-PIN photodiode (-55 °C).
internal multilayer collimator- to minimize background and spectral artifacts.

The energy resolution - from 139 to 190 eV FWHM@ 5.9 keV (depending on the detector area).
It is best - at count rates below 30 kcps.
It is suited to X-rays between 1.5 and 30 keV.
It uses a fully depleted 500 um Si-PIN photodiode.
It is available with 1 or 0.5 mil Be windows.

Detection Limit

a) It determined by the BG of the X-rays spectrum.
b) The main BG components produzed by proton impact is:

For Ep < 1.5 MeV- AB.
For 1.5 MeV- 2 MeV, AB+SEB
For Ep>3MeV, SEB+Compton tail BG of gamma rays.

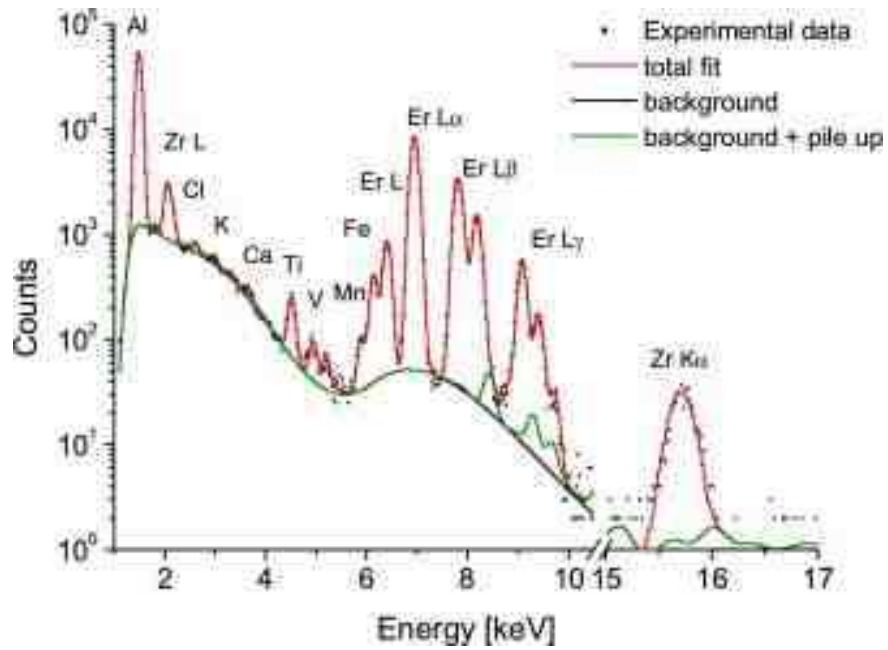

PIXE intrinsic detection limit (DL) is not very much below 1 ppm (mg kg^{-1}) in a given matrix. It offers its maximum sensitivity in two atomic number (Z) regions: 20 < Z < 30 and 75 < Z < 85. Measurement errors are in the order of 10%, depending mainly on the target preparation procedure and on the slight variability of the proton flux.

Experimental setup

The X-ray detection system, housed in the vacuum chamber, is generally a Si(Li) device, that combines the advantage of high efficiency in the X-ray energy region of interest (usually 2–20 keV) with a good energy resolution.

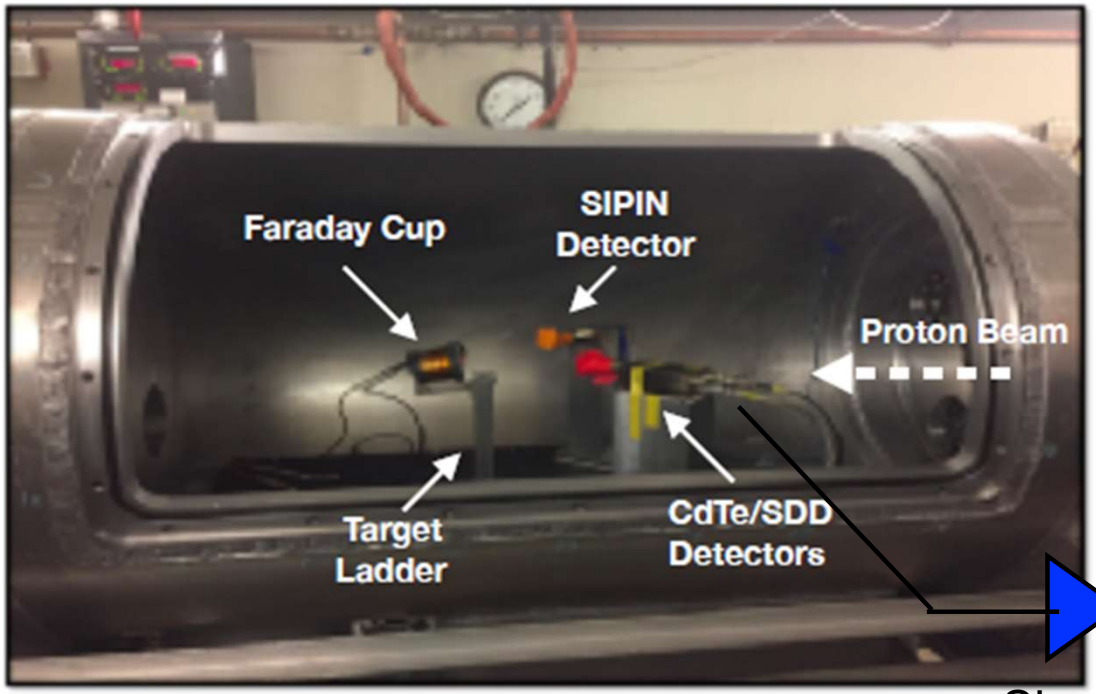

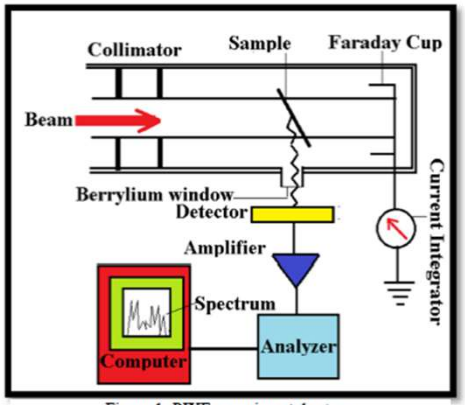

Figure 1: PIXE experimental set up.

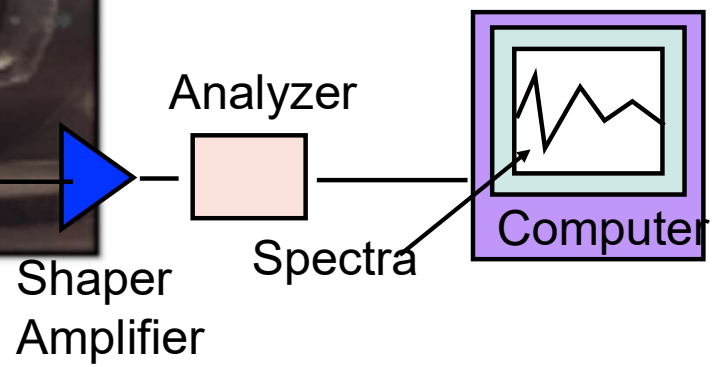

Sample preparation

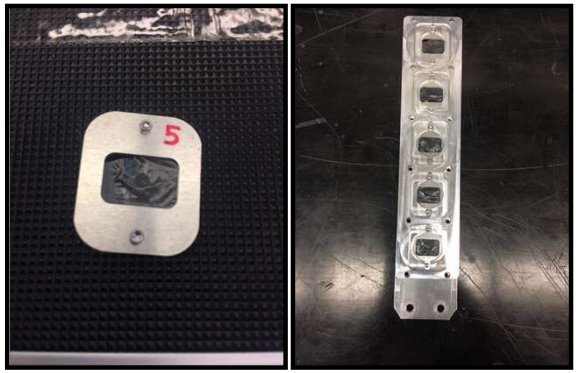

Target Ladder

Sample Preparation

Powders:

Grinding (<400 mesh if possible) can minimise scatter affects due to particle size. Additionally, grinding insures that the measurement is more representative of the entire sample, vs. the surface of the sample.

Pressing (hydraulically or manually) compacts more of the sample into the analysis area, and ensures uniform density and better reproducibility..

Solids:

Orient surface patterns in same manner so as minimise scatter affects.

Polishing surfaces will also minimise scatter affects.

Flat samples are optimal for quantitative results.

Liquids:

Samples should be fresh when analysed and analysed with short analysis time - if sample is evaporative.

Sample should not stratify during analysis.

Sample should not contain precipitants/solids, analysis could show settling trends with time.

Analysis

Qualitative

Quantitative

Absolute

Comparison Method

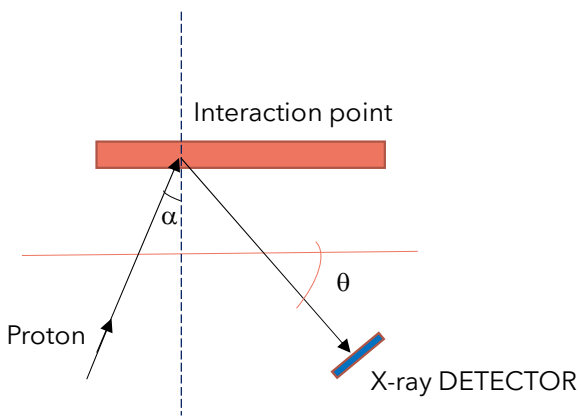

Quantification for thin target.

$$N_{\upsilon} = \left(\frac{\Omega}{4\pi} . \varepsilon_{\upsilon}\right) . N_p . n_Z \ \sigma_{\upsilon}$$

Where:

N_{υ}(Z)-the number of counts bellow the peak of characteristic X-rays (υ-line) for an element (atomic number- Z), obtained from spectra.

Ω -solid angle subtended by the X-ray detector at the target.

ε_{υ}-detection efficiency for the υ-line of x-ray.

σ_{υ}-production cross section for υ-line x-rays of element Z.

N_p- Number of incident protons that hit the sample.

n_Z —number of atoms per unit area at the sample of the element Z.

$$n_Z = \frac{N_{AV} . m_Z}{A_Z}$$

With, N_{AV}- is the Avogadro's Number; m_z- is the quantity of interest (areal concentration- [mass/area]) and A_Z- Atomic mass of the sample element.

How measure N_p- Number of incident protons that hit the sample?

Protons are positively charged; and we know the charge carried by a proton (1,60210. 10^{-19} C).

Therefore, the charge carried by N_p protons is

$$Q_p, [\mu C] = 1{,}60210.\ 10^{-13}.\ N_p$$

. Direct Measurements (FARADAY CUP+ charge integrator coupled directly to cup- thin samples, or , the integrator is coupled directly to holder of specimen for thick or conducting samples)

. Indirect measurements (RBS in carbon backing)

About σ_{υ} - production cross section for υ-line x-rays of element Z.

Theoretical determination:

_The binary encounter approximation (BEA)

_The semi-classical Approximation (SCA)

_The Plane Wave Born Approximation (PWBA). ♥

PWBA has a good agreement with experimental data for K-shell, but for L- shel ionization the situation is much less favorable.

$$\sigma_{\upsilon} = \sigma_S . w_S . r_{\upsilon}$$

Where:

σ_S- Inner ionization cross section (S=K, L, M,..). probability of an electron is being removed of the shell by a proton impact.

w_S - fluorescence yield.

r_{υ}-fractional radiative width of υ-line X-rays.

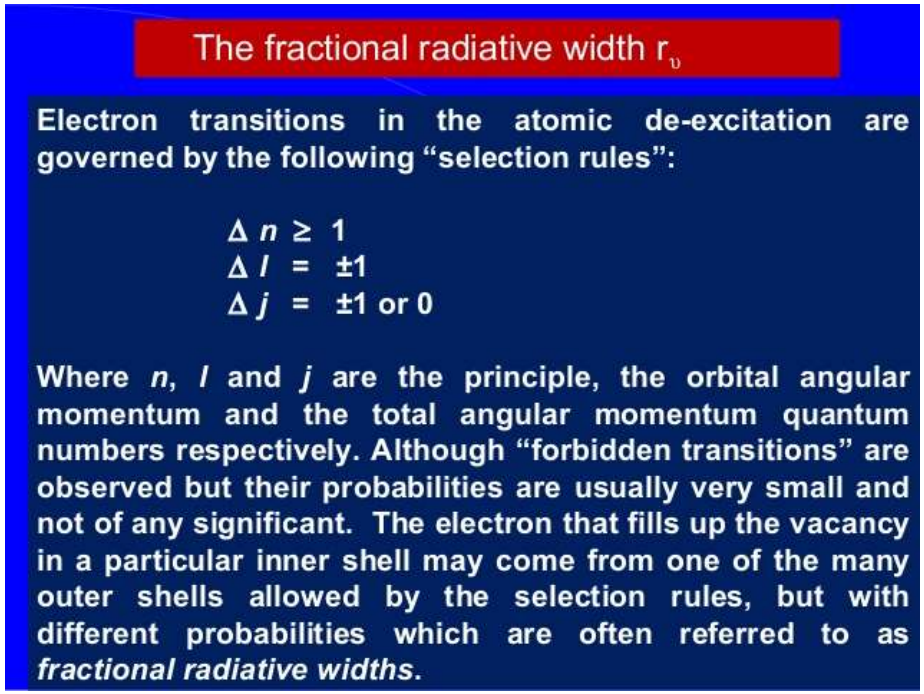

Detection efficiency ε_ν

The detection efficiency of a Si(Li) X-ray detector is dependent on the X-ray energy. It is usually determined theoretically using the parameters (i.e. thicknesses of Si diode, Be window, gold contact and Si dead layer) provided by the detector manufacturer. However, calibration standards are often used to determined ε_ν experimentally.

Si-PIN Detection Efficiency

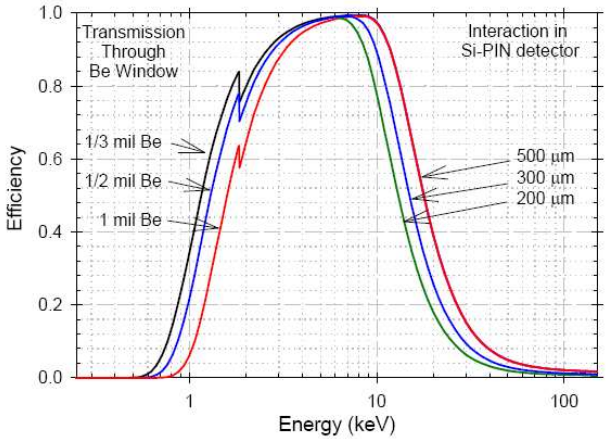

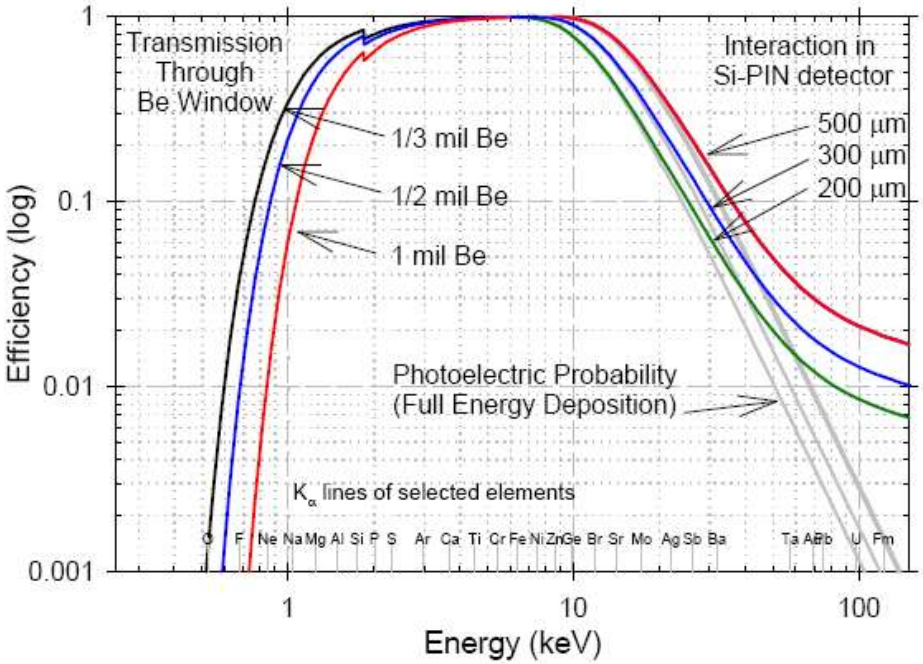

Si-PIN: Recommended for applications requiring moderate energy resolution and count rate, where cost is most important. Si-PIN devices have a conventional planar structure, yielding more electronic noise than an SDD but are easier to fabricate. There are three different Si-PIN variations currently available, with areas of 6 mm2, 13 mm2, and 25 mm2. The 6 mm2 detectors provide an energy resolution of 140 eV FWHM at the 5.9 keV Mn Ka line at count rates up to 50k cps. The 13 mm2 and 25 mm2 detectors typically offer energy resolutions of 180 and 210 eV FWHM for the same count rates.

$$m_Z[\frac{g}{cm2}] = (\frac{4\pi}{\Omega})(\frac{1}{\varepsilon_\upsilon})(\frac{e}{Qp})(\frac{N_\upsilon}{\sigma_\upsilon})(\frac{A}{N_{AV}})$$

In the PIXE measurements of intermediate and thick samples, the bremsstrahlung BG can be large, especially in low energy region.

Therefore, we found POOR detection limits mainly for Light elements as well as diminish the sensitivity for the detection of intermediate and high Z elements.

Due that, plastic or metal filters of appropriated thickness are often placed between specimen and the detector (it reduces considerably the BG at low energy region).

Now we need correct the expression for the areal concentration, by this transmission factor which is function of the energy.

$$m_Z[\frac{g}{cm2}] = (\frac{4\pi}{\Omega})(\frac{1}{\varepsilon_\upsilon})(\frac{e}{Qp})(\frac{N_\upsilon}{\sigma_\upsilon})(\frac{A}{N_{AV}})\ (\frac{1}{f_t})$$

Internal Standard Method.
External Standard Method.

$$m_Z[especimen] = (\frac{4\pi}{\Omega})(\frac{1}{\varepsilon_\upsilon})(\frac{e}{Qp})(\frac{N_\upsilon}{\sigma_\upsilon})(\frac{A}{N_{AV}})\ (\frac{1}{f_t})$$

Unknown efficiency

$$\frac{m_Z[especimen]}{m_Z[standard]} = \frac{N_X(specimen)}{N_X(standard)}$$

Analysis software, GUPIXwin (J.L Campbell, from Guelph)

Quantitative Analysis

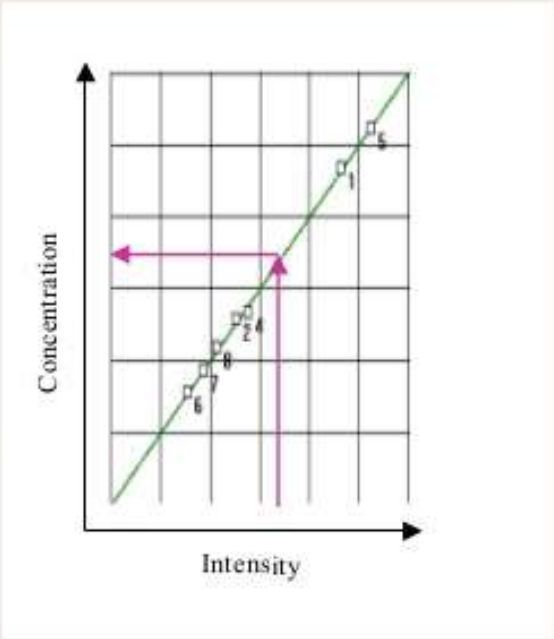

XRF is a reference method, standards are required for quantitative results.

Standards are analysed, intensities obtained, and a calibration plot is generated (intensities vs. concentration).

XRF instruments compare the spectral intensities of unknown samples to those of known standards.

GUPIX

- Fit model-to-measure spectra demands knowledge of x-ray line intensities database and modifications (relative to intrinsic values) by matrix effects.
- all peak energies and peak intensities have a data base of:
- energy lines and branching ratios
- production cross-sections
- fluorescence
- proton stopping powers
- attenuation coefficients
- elemental densities
- atomic weights

Applications

Biological samples: The sensitivity of PIXE analysis to H, C, N, and O is very low due to absorption in the detection window (usually Be film) of X-ray detectors. However, it is very high in the case of absorption of metallic elements and heavy elements in biological samples consisting of light elements as the main ingredients.

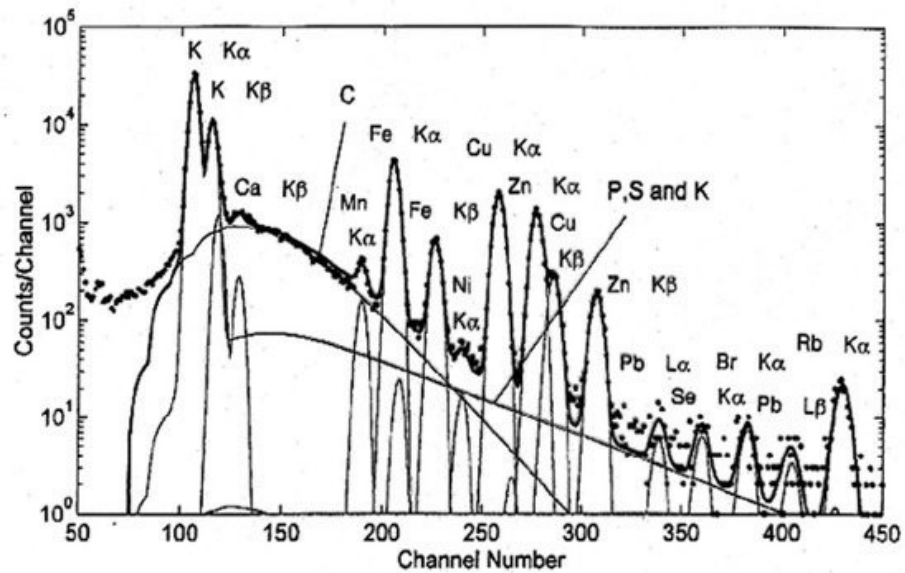

Peak separation of an X-ray energy spectrum of bovine liver obtained using 3 MeV proton PIXE. The continuous background in this figure consists of SEB and AB from carbon, phosphorus, sulfur and potassium.
Peak fitting software is commercially available, such as GUPIXWIN (University of Guelph, Guelph, ON, Canada).

Murozono K.et al. PIXE spectrum analysis taking into account bremsstrahlung spectra. Nuclear Instrument and Method. Phys. Res B 1999, 150, 76-82

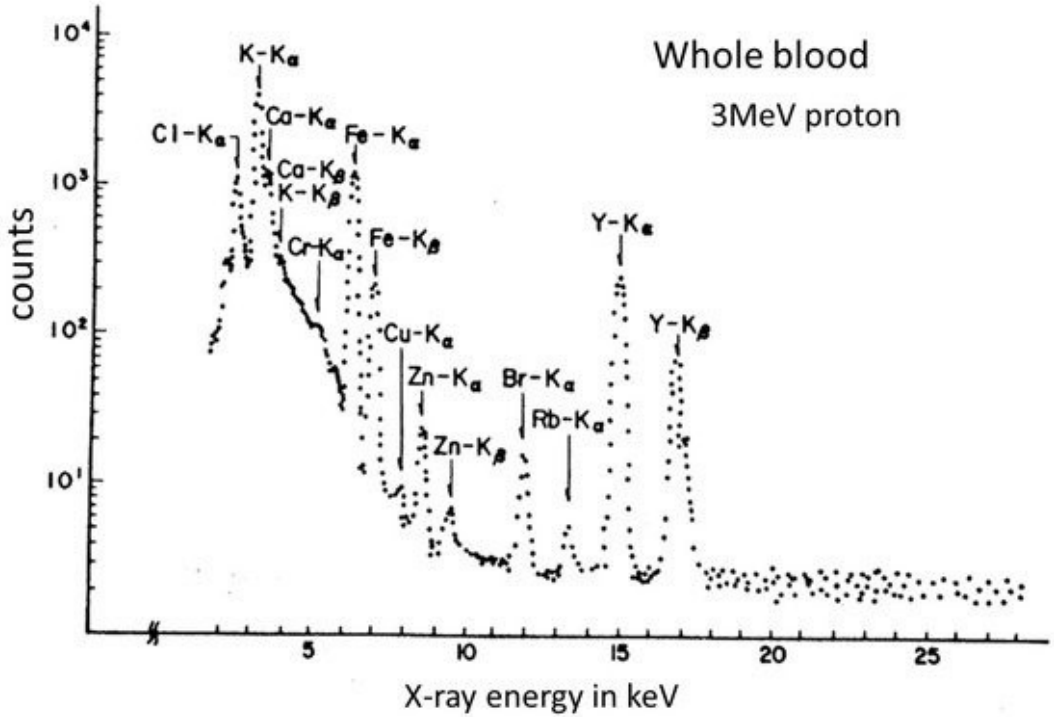

PIXE spectrum of the whole blood of a healthy person.

The peaks of the elements Na, P, S, K, Cl, Ca, Cr, Fe, Cu, Zn, Br, and Y were observed in this spectrum.
The Y element was contaminated in the sample as a standard element.
Research revealed that changes in the concentrations of metallic elements in the blood are strongly related to aging and illness.
Changes in the concentration of Zn are strongly related to disease.
It seems that the concentration ratio, Cu/Zn, of Cu and Zn in blood is also closely related to health conditions.
The results of PIXE analysis in the blood of leukemia patients showed that the concentration ratio of Cu/Zn was four times larger than that of normal people.
It has also been reported that chronic articular rheumatism affects the concentration ratios of elements .

Ishii K., et al. Quantitative trace-Element analysis by proton-induced X-rays. Nucl. Instr. Meth. 1975, 126, 75-80.

Characterize elemental composition of thin films of poly-dialydimethyl-amonium-cloride and poly-styrene-sulfonate.
Alis Rodriguez Manso/Cyclotron Lab of TAMU/USA. CAARI 2018. 25th Intern.Conference the Appl. Of Accelerators in Research and Industry.

- Pilot experiment using the K150 cyclotron
- Matrix bombarded with a 3.6MeV p. beam, intensity ~ 2nA and beam spot size of 5-10mm
- Resulting x/ɣ-rays measured with **SiPIN**, SDD and CdTe detectors
- At 45^0 with respect to beam direction.

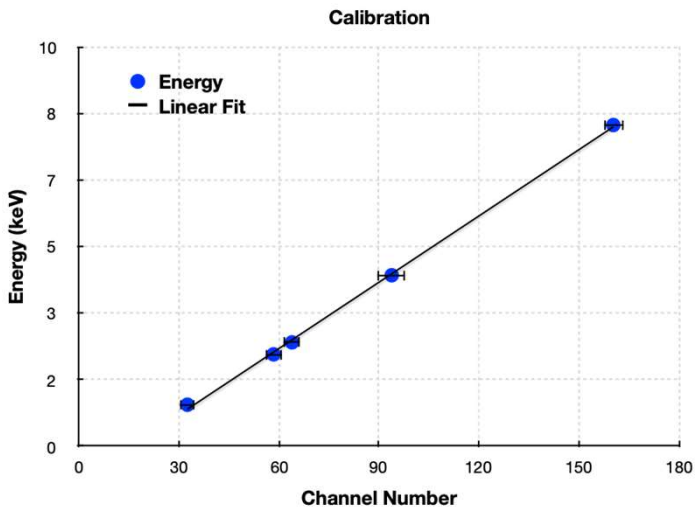

*E(Channel) = 0.055eV *Channel - 0.878eV*

Si-pin detector calibration. Various peaks from the CsBr, KCl, InS and NaCl standards were used.

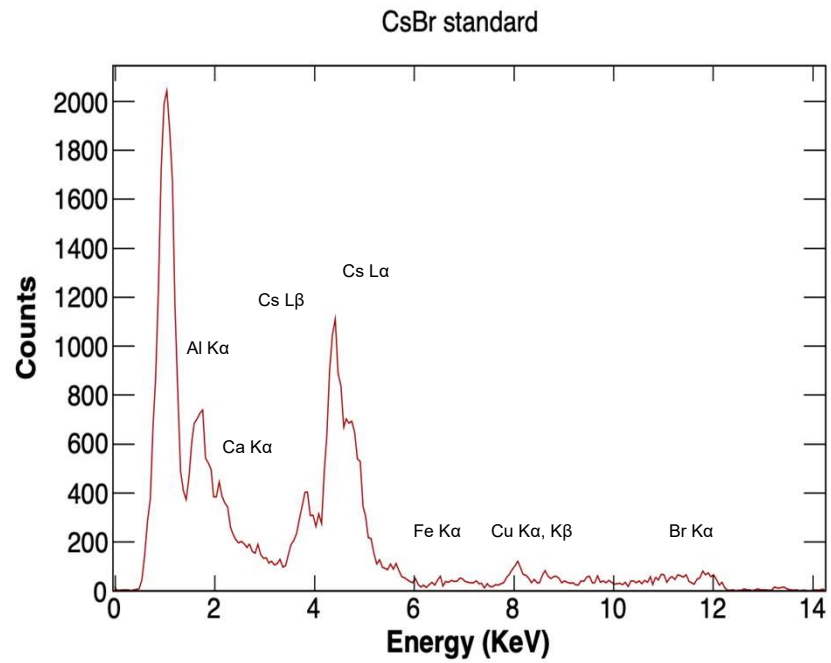

CsBr standard, which noticeable elements include Al, Cs, Ca, Fe, Cu and Br.

Environmental Samples.

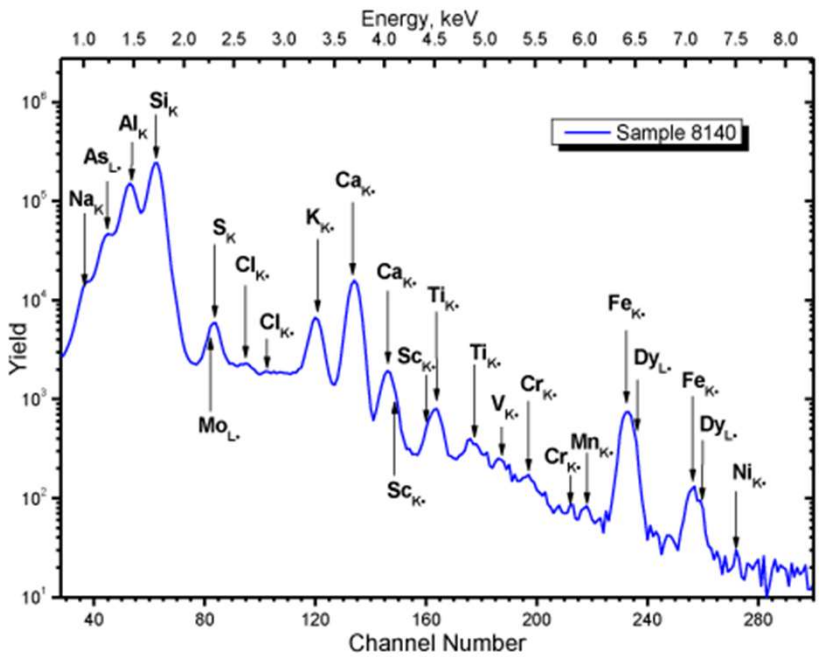

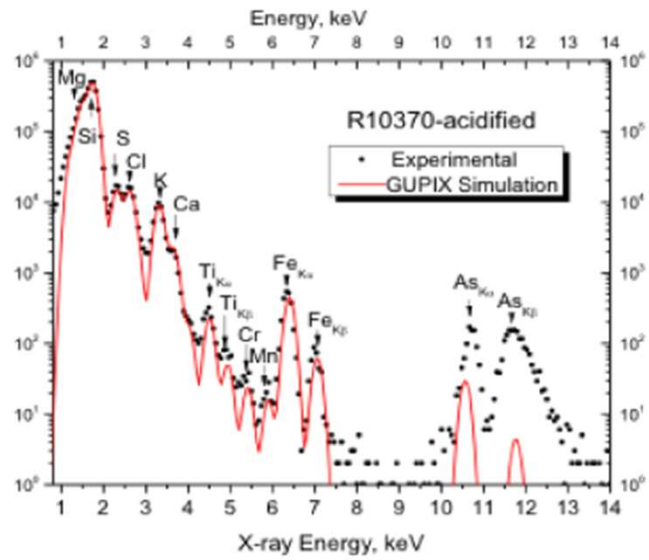

Example of PIXE analysis of Shale (sedimentary rock) yielded a large range of elemental concentrations. Spectra are normally analyzed by comparison with a simulated spectrum (as shown by the red spectrum on the right.)

Air Sample.

Mohri M., et al.Bulletin of Faculty of Engineering on Hokkaido University, Japan, 1983, vol 114: PIXE spectrum of airbone dust in Sapporo, Japan in April 1982

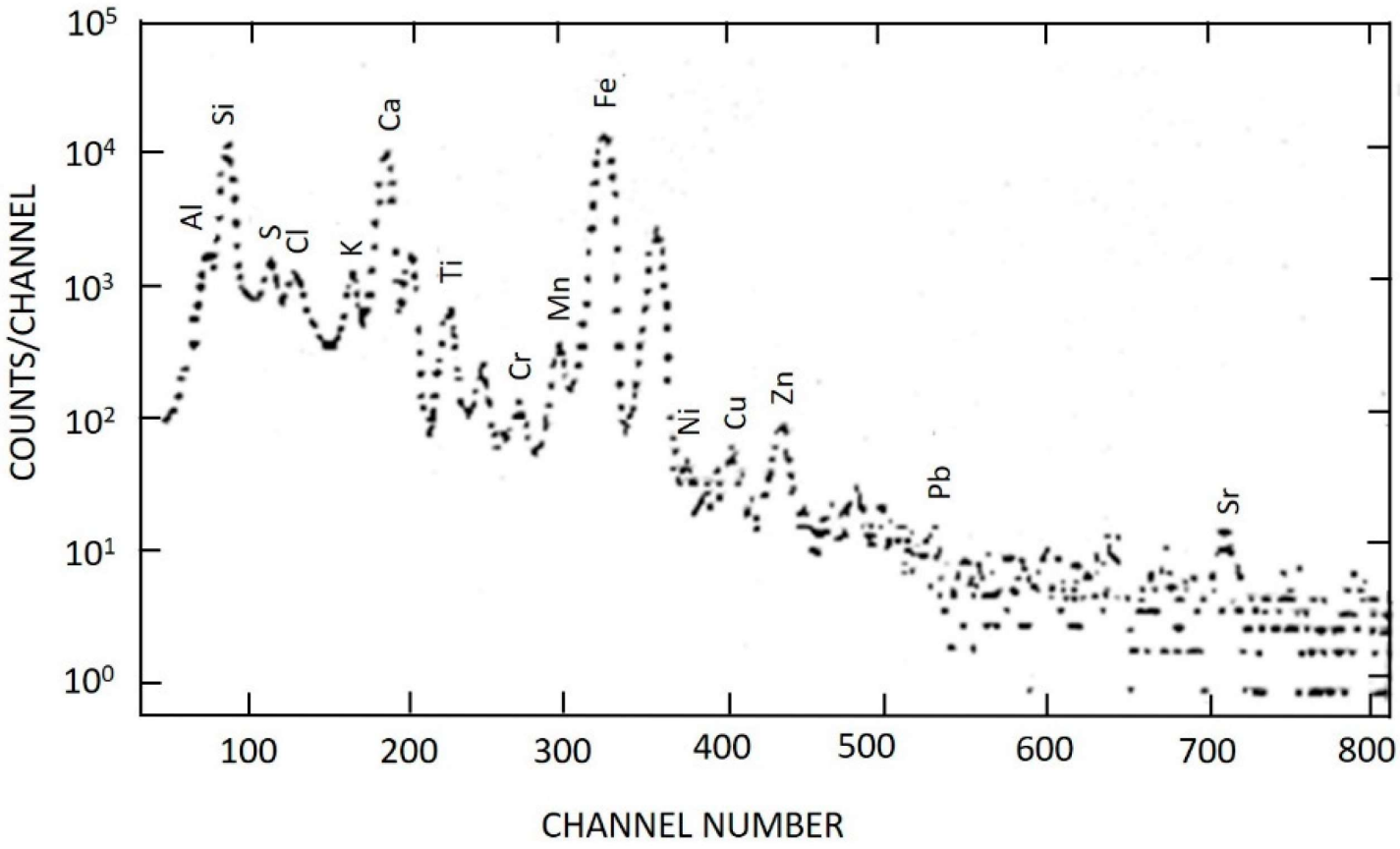

PIXE, RBS and ICP-MS Analysis of a Moche Archeological Artifact: Manfredo H. Tabacniks Instituto de Física USP. J. Phys. D. Applied Phys. 36 (2003) 842-48.

- PIXE Particle Induced X-Ray Emission
- Concentração absoluta (at/cm2)
- Alcance (feixe com 2MeV): H+ ~30μm
- Sensibilidade < 1012 Au/cm2 ou ~ppm bulk
- Alta resolução para elementos vizinhos
- Rápido (~10min)

PIXE - Example: Prussian Medal

- Prussian Medal, about 1790
  Deutsches Historisches Museum, Berlin
- massive object?
  gilded?
- t = 200s,
  I_p ~0.1 pA
- result:
- medal:
  $L\alpha/K\alpha$ = 1.09

  1 μm Au-foil:
  $L\alpha/K\alpha$ ~ 40,

  ~ 75% Au
  ~ 15% Ag
  ~ 10% Cu

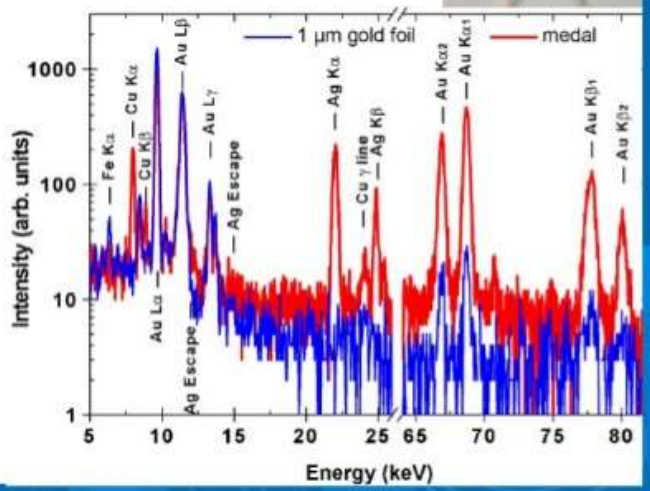

Fake or Forgery?

The art market is flooded with fake paintings of 20th century artists such as ... Matisse, Modigliani, Picasso ...

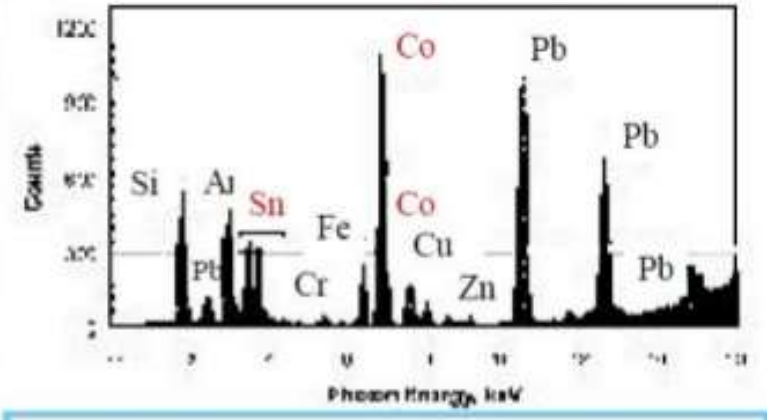

X-ray spectrum indicated the use of cerulean blue $CoO \cdot n \cdot SnO_2$ a pigment Modigliani did not use in any other of his paintings ⇒forgery?

Final remarks

PIXE: Particle Induced X-ray Emission

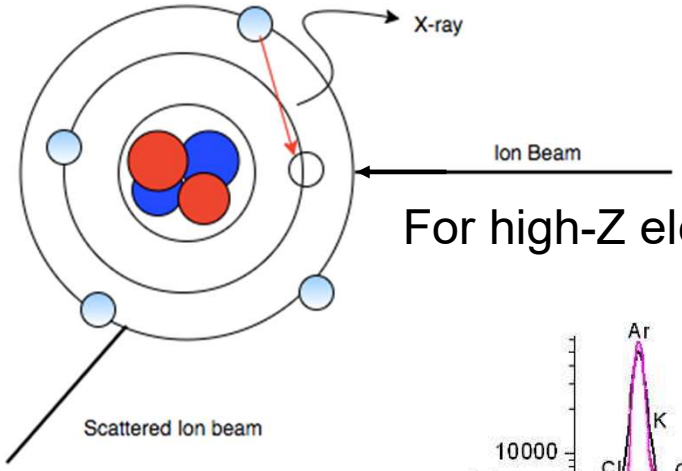

For high-Z elements

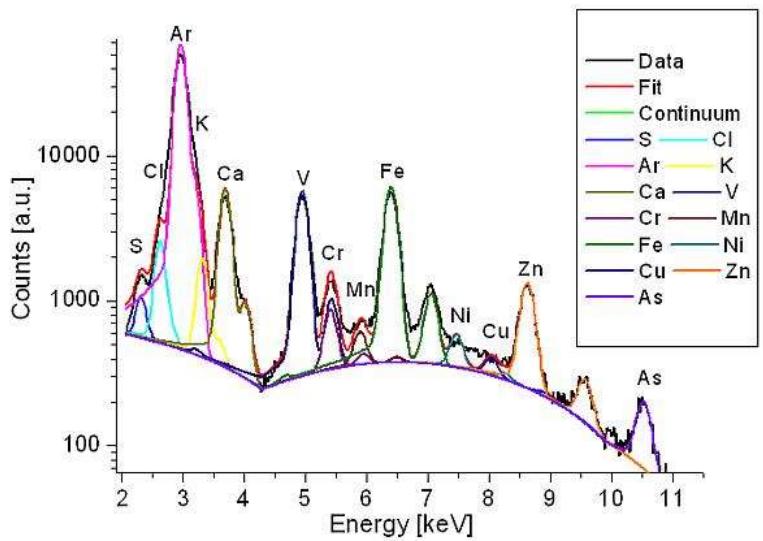

- Multi-elemental
- Quantitative analysis
- High sensitive
- Non destructive
- Non sample pre-treatment
- Quick

References.

1. Johanson, S.A.E; Campbell, J.L. PIXE:A novel technique for elemental Analysis; John Wiley & Son: Hoboken, NJ, USA, 1988.
2. Johansson, T.B.; Akselsson, R. SAE Johansson X-ray analysis: elemental trace analysis at the 10–12g level Nucl. *Instr. Meth.* **1970**, *84*, 141–143.
3. Garcia, J.D. Inner-shell ionizations by proton impact. *Phys. Rev. A* **1970**, *1*, 280–285.
4. Hansteen, J.M.; Mosebekk, O.P. Atomic Coulomb excitation by heavy charged particles. *Nucl. Phys. A* **1973**, *201*, 541–560.
5. Lewis, H.W.; Simmon, B.E.; Merzbacher, E. Production of characteristic X-rays by protons of 1.7-to 3-Mev energy. *Phys. Rev.* **1953**, *91*, 943.
6. Brandt, W.; Laubert, R.; Sellin, I. Characteristic X-ray Production in Magnesium, Aluminum, and Copper by Low-Energy Hydrogen and Helium Ions. *Phys. Rev.* **1966**, *151*, 5.

7. Brandt, W.; Lapiki, G. Energy-loss effect in inner-shell Coulomb ionization by heavy charged particles. *Phys. Rev. A* **1981**, *23*, 1717.

8. Cohen, D.D.; Harrigan, M. K-and L-shell ionization cross sections for protons and helium ions calculated in the ECPSSR theory. *At. Data Nucl. Data Tables* **1985**, *33*, 255.

9. Paul, H.; Sacher, J. Fitted empirical reference cross sections for K-shell ionization by protons. *At. Data Nucl. Data Tables* **1989**, *42*, 105.

10. Johansson, E.M.; Johansson, S.A.E. PIXE analysis of water at the parts per trillion level. *Nucl. Instr. Meth. B* **1984**, *3*, 154–157.

11. Mandó, P.A. Advantages and limitations of external beams in applications to arts & archeology, geology and environmental problems. *Nucl. Instr. Meth. B* **1994**, *85*, 815–823.

12. Murozono, K.; Ishii, K.; Yamazaki, H.; Matsuyama, S.; Iwasaki, S. PIXE spectrum analysis taking into account bremsstrahlung spectra. *Nucl. Instr. Meth. Phys. Res. B* **1999**, *150*, 76–82.